Towards Adaptive Kinetic-Fluid Simulations of
Weakly Ionized Plasmas

Vladimir Kolobov and Robert Arslanbekov

Semicon West
San Francisco, CA
July 14, 2011

Agenda

- **Plasma Technologies and Plasma Models**
- **Commercial Software for Plasma Simulations**
- **Simulations of industrial plasma reactors for semiconductor manufacturing with CFD-ACE+**
- **Evolution of Mesh Technologies: from Body-Fitted to Cartesian Mesh**
- **Adaptive Mesh Refinement (AMR) using Octree Cartesian mesh**
- **Unified Flow Solver and AMAR technology for multi-scale kinetic-fliud simulations of gas flows in the transitional regimes**
- **Plasma Simulations with AMR**
- **Conclusions**

Plasma Technologies

"The XXI century will be not only the century of informatics, biology and space exploration, but also the century of plasma technologies" A.I.Morozov 2006

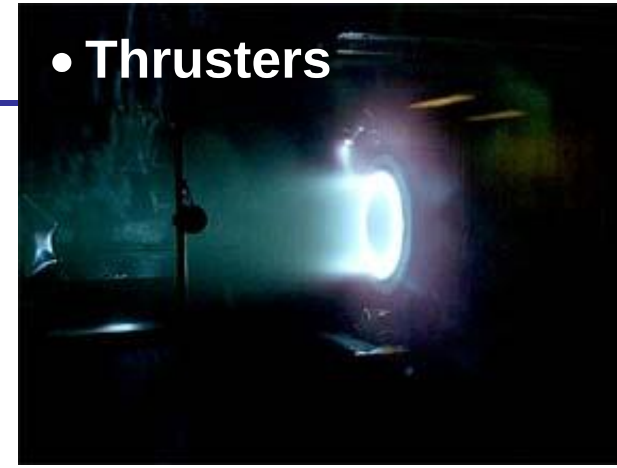

- Thrusters

- Lighting

- Spray Coatings

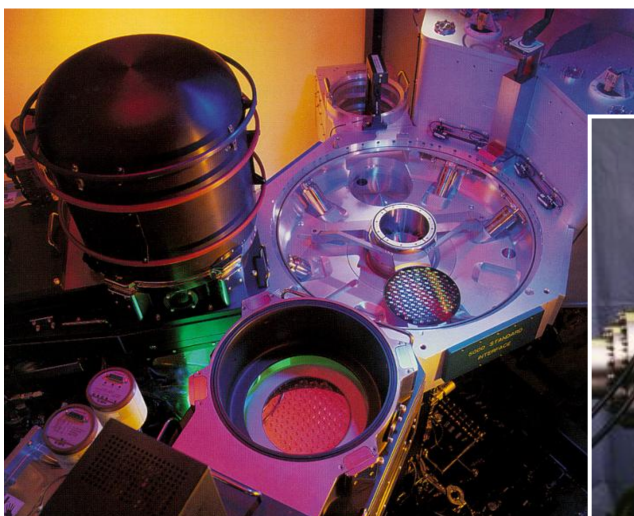

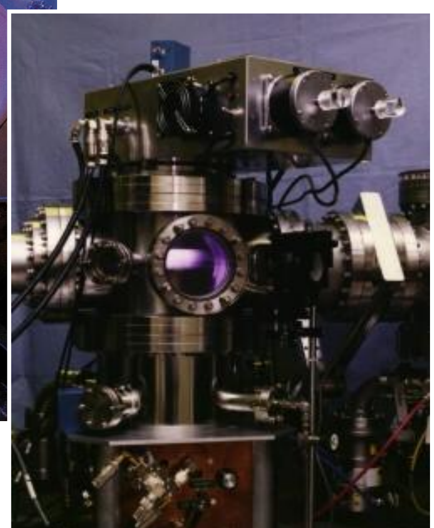

- Materials Processing

- Displays

Plasma Models

Different plasma models are currently used for modeling thermal and non-equilibrium plasmas

High Pressure Thermal Plasmas

- $T_e = T$, LTE
- Gas Flow (turbulence)
- Heat Transfer
- Radiation (HF EMAG)

- Non – Equilibrium Chemistry
- Two Temperature $T_e \geq T$

Key Features

- Radiation Transport
- Gas Heating $T > T_{room}$

Low Pressure Non-Equilibrium Plasmas

- Magnetic Field Effects
- Kinetics of Ions & Fast Neutrals
- Kinetics of Electrons
- Non-Local Electrodynamics

The need to develop new modeling techniques that address vastly different scales having different physics at both low and high pressures speaks to the convergence of the discipline

Commercial Software for Plasma Simulations

CFDRC developed the first commercial tool for plasma simulations

In 2004, CFD-ACE+ software was sold to ESI group.

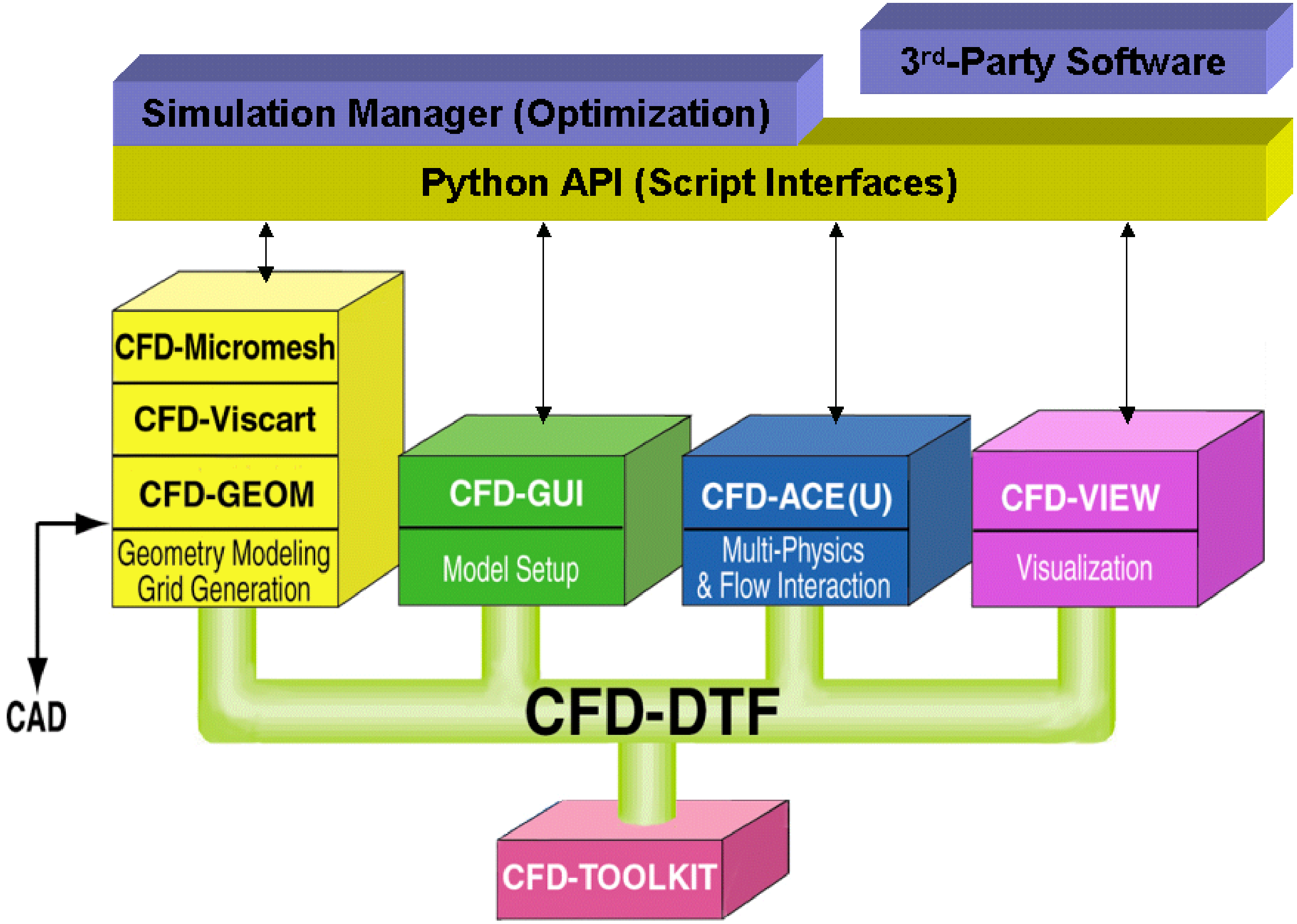

Plasma Simulations with CFD-ACE+

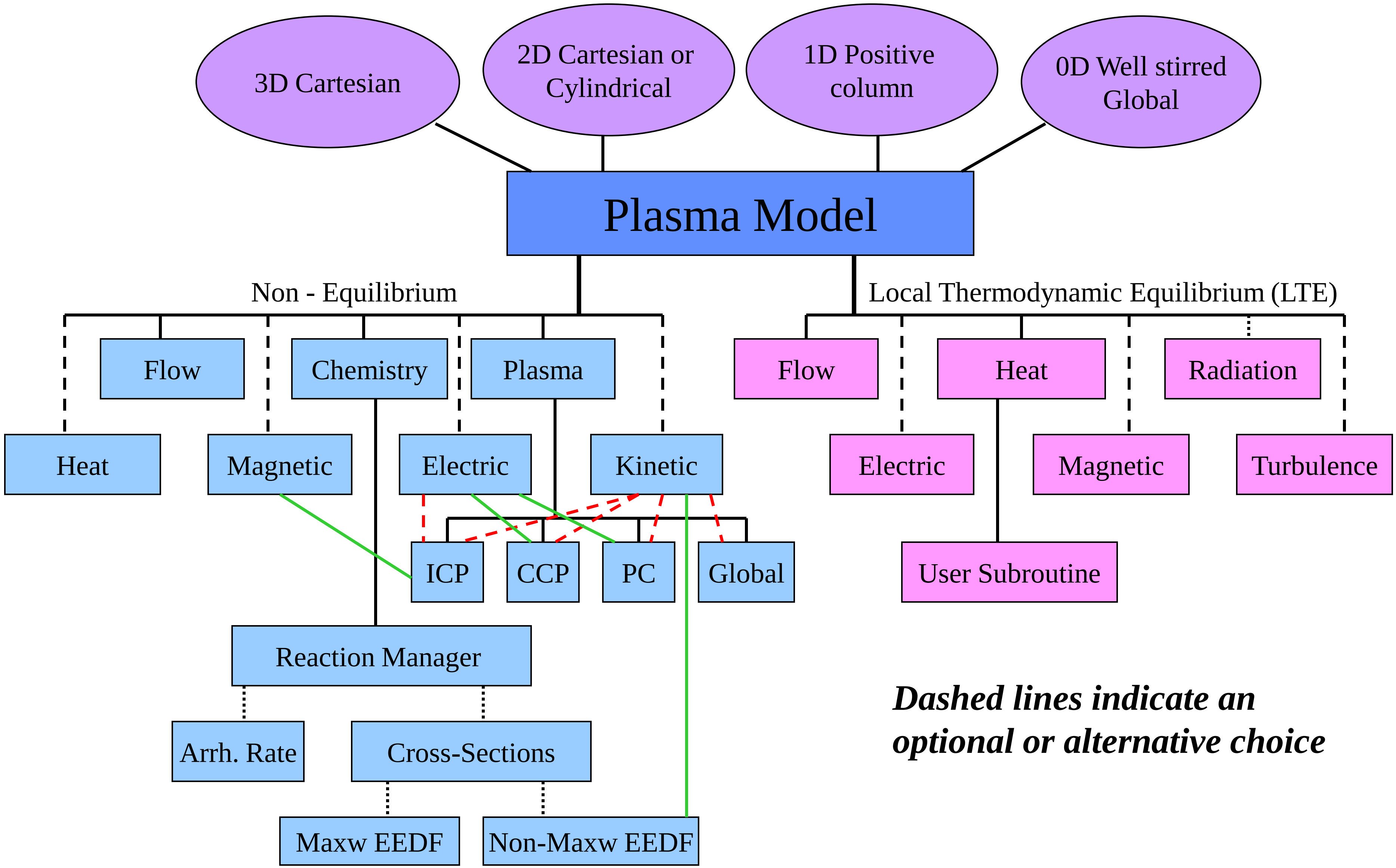

Dashed lines indicate an optional or alternative choice

Inductively Coupled Plasma Reactors

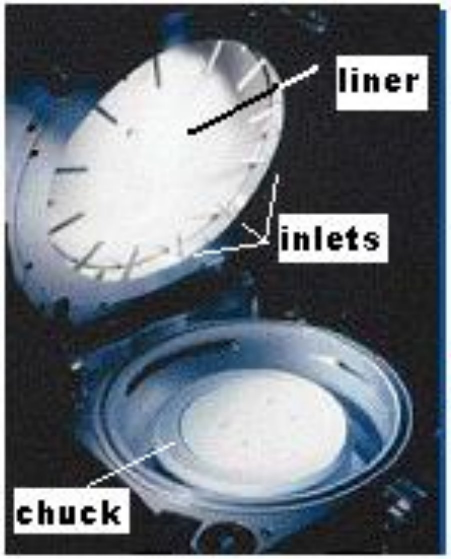

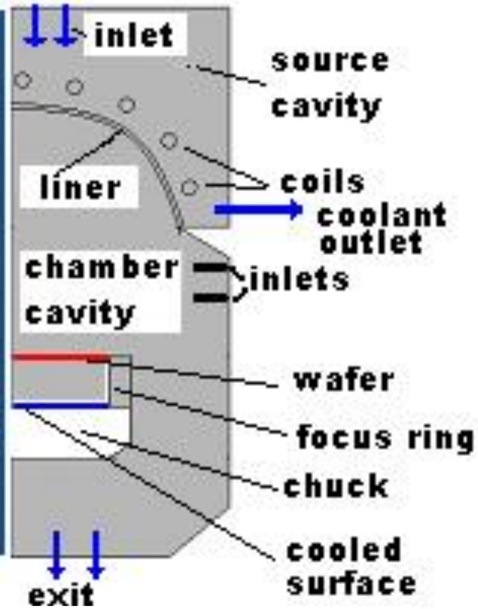

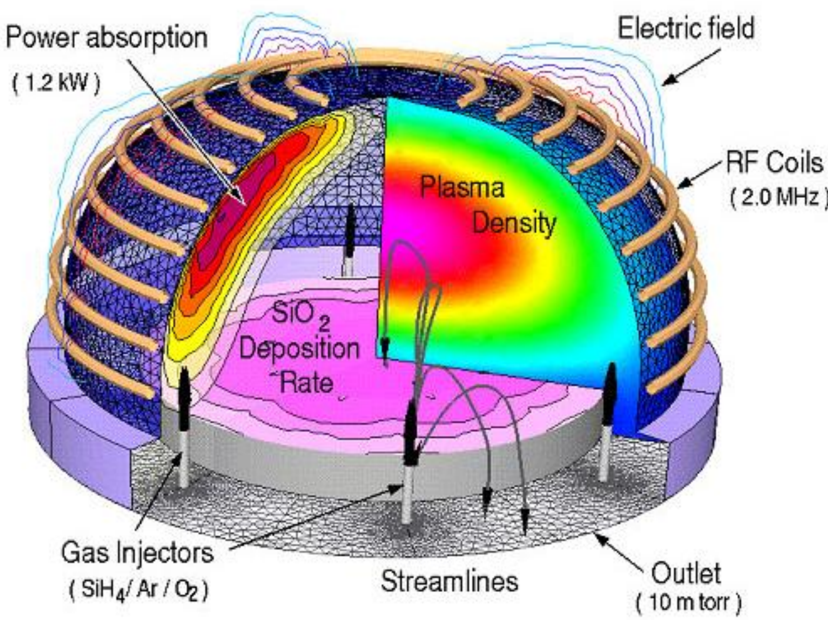

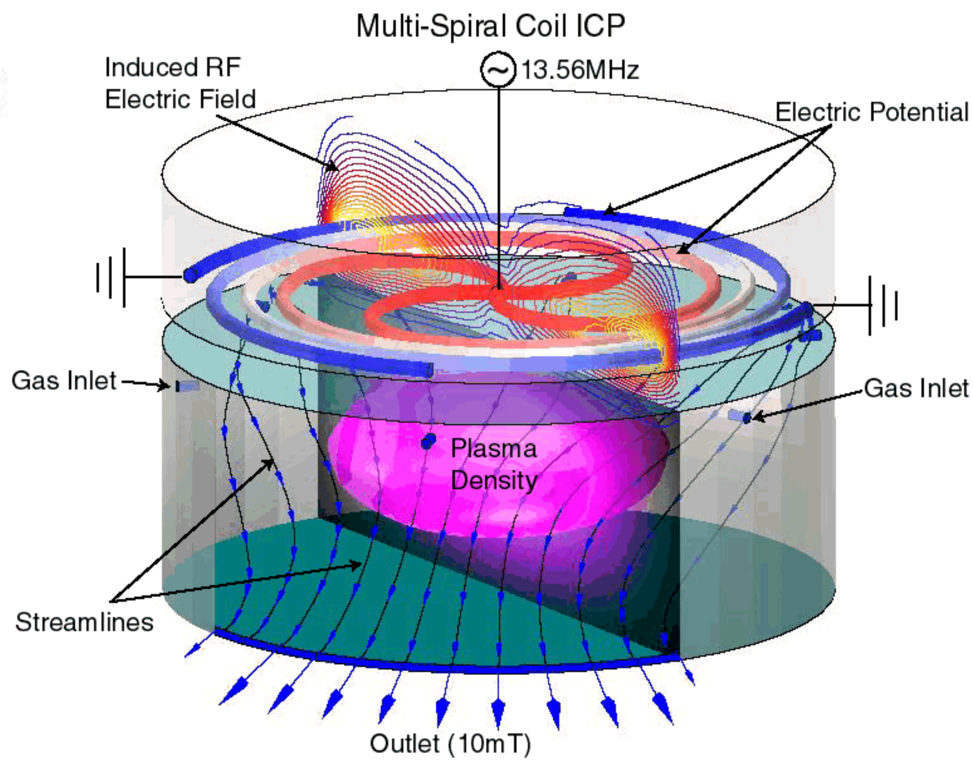

Capacitively Coupled Plasma Reactor

CFD-ACE+ 3D Simulation of Capacitively Coupled Plasma

(400 mTorr, Oxygen)

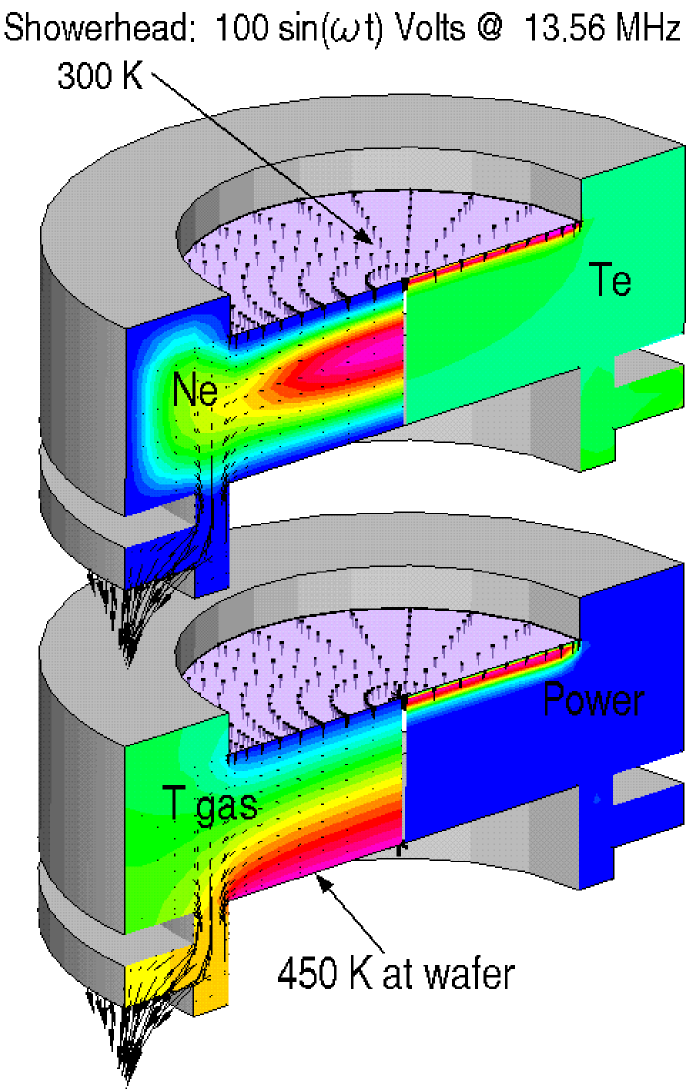

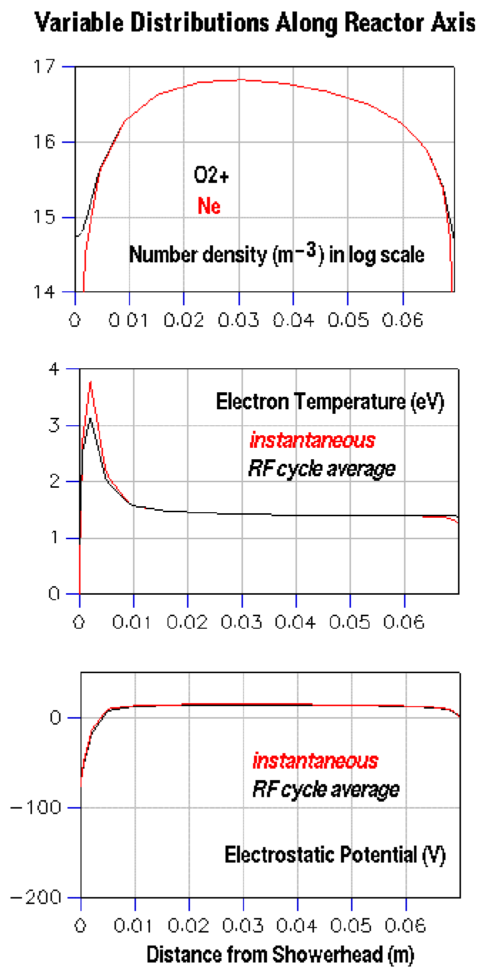

- Multi-frequency electrodes
- Coupled plasma and gas dynamics simulations
- External Circuit models
- Complex gas and surface chemistry
- Parallel Capabilities

Electron Kinetics

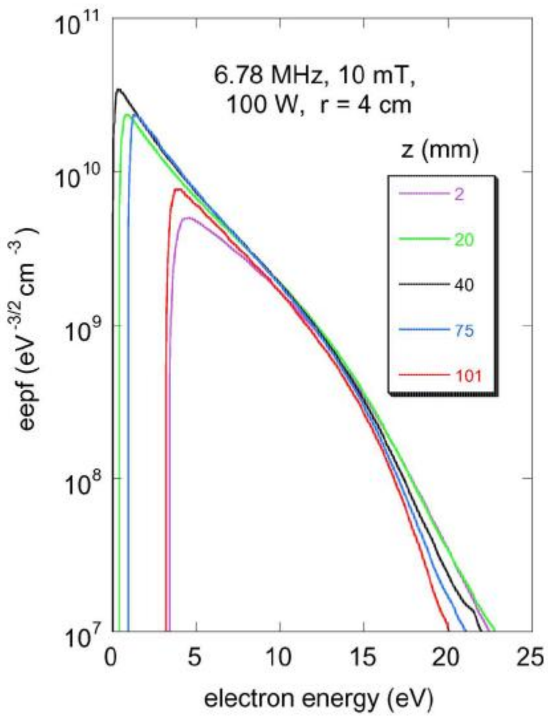

(a)

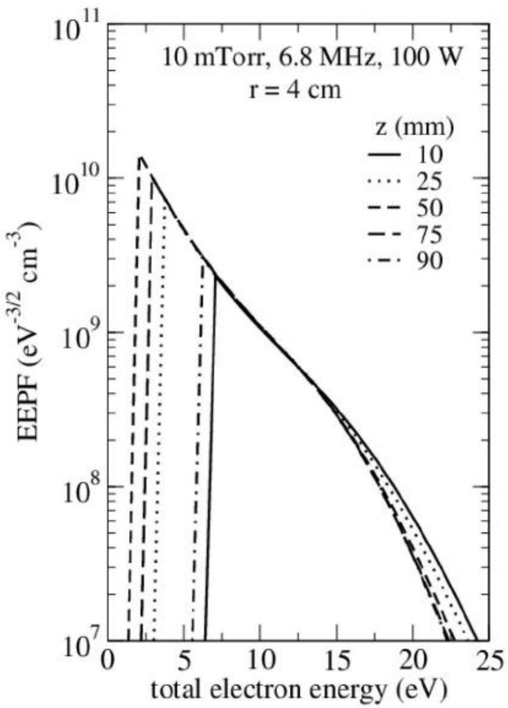

(b)

EEPFs at different points along the discharge axis at radial position *r*=4 cm: a) measured, b) calculated.

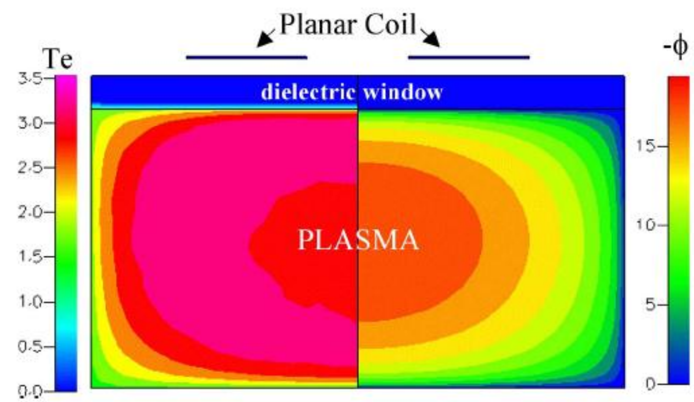

Calculated electron temperature (left) and electrostatic potential (right) for Ar ICP at 10 mT, 6.8 MHz, 100W.

$$\frac{\partial f_0}{\partial t} + \frac{\mathrm{v}}{3}\mathrm{div}(\mathbf{f}_1) + \frac{1}{3\mathrm{v}^2}\frac{\partial}{\partial \mathrm{v}}\left(\mathrm{v}^2 \frac{e\mathbf{E}}{m}\cdot \mathbf{f}_1\right) = S_0$$

$$\frac{\partial \mathbf{f}_1}{\partial t} + \nu \mathbf{f}_1 = -\mathrm{v}\nabla f_0 - \frac{e\mathbf{E}}{m}\frac{\partial f_0}{\partial \mathrm{v}}$$

Two-term SHE reduces 6D Boltzmann equation to a 4D Fokker-Planck equation for electrons in collisional plasmas

$$\mathbf{f}(\mathbf{r},\mathbf{v}.t) = f_0(\mathbf{r},\mathrm{v},t) + \frac{\mathbf{v}}{\mathrm{v}}\cdot \mathbf{f}_1(\mathbf{r},\mathrm{v},t)$$

Using total energy (kinetic + potential) simplifies analysis

of electron kinetics for many gas discharge problems

$$\frac{\partial f_0}{\partial t} - \frac{\partial \phi}{\partial t}\frac{\partial f_0}{\partial \varepsilon} - \nabla\cdot D_r \nabla f_0 - \frac{1}{\chi}\frac{\partial}{\partial \varepsilon}\left(\chi\left[D_\varepsilon(\mathbf{r},\varepsilon)\frac{\partial f_0}{\partial \varepsilon} + V_\varepsilon(\mathbf{r},\varepsilon) f_0\right]\right) = S$$

V. Kolobov & R. Arslanbekov, Simulation of Electron Kinetics in Gas Discharges, IEEE TPS 34 (2006), 895

Pattern Formation in DBD

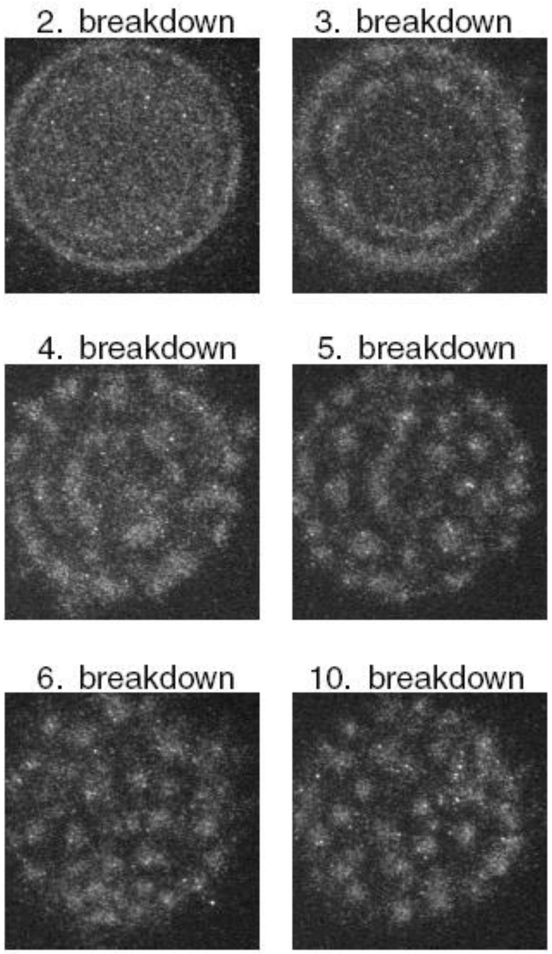

Experimental measurements of pattern formation dynamics in He DBD 200kHz, 30kPa, 690 V. Stollenwerk et al. Phys. Rev. Letters 96 (2006) 255001

Our simulations: fluid model with LUTs

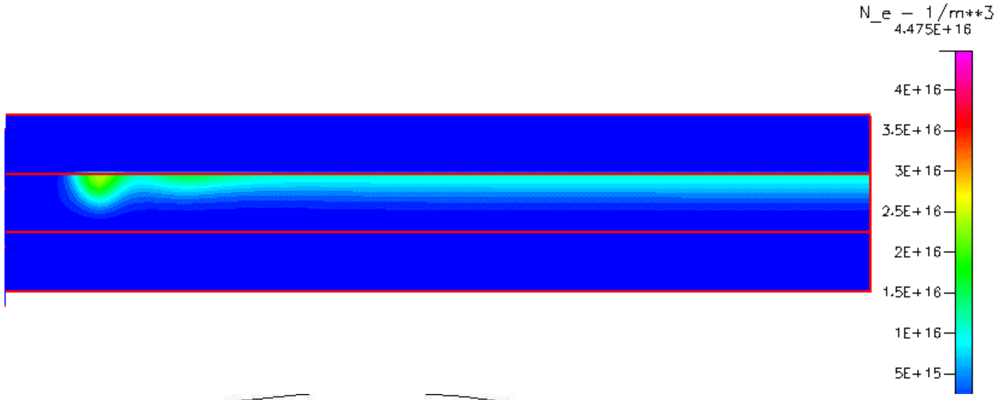

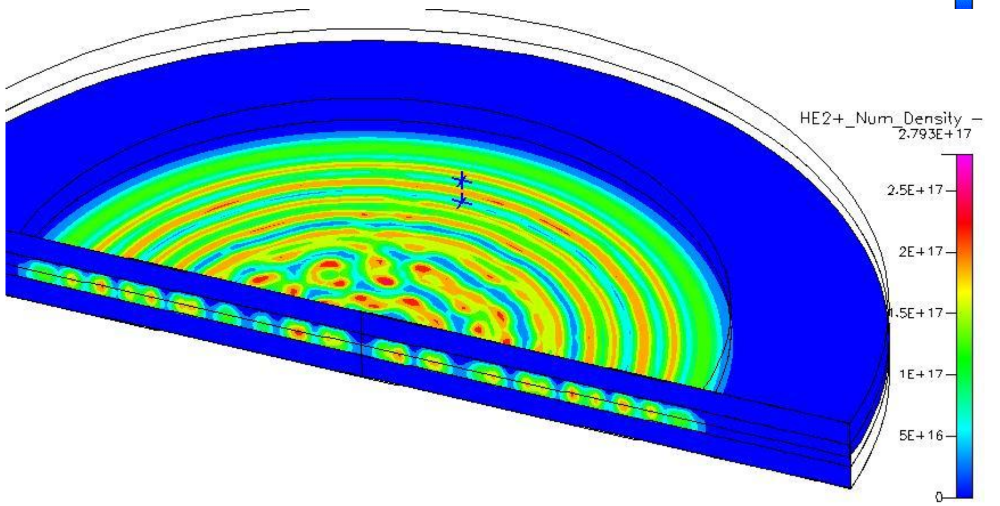

Open questions

- Effect of computational mesh
- Operating conditions (gas, pressure, voltage)
- Electrode resistivity

Summary about plasma simulations with CFD-ACE+

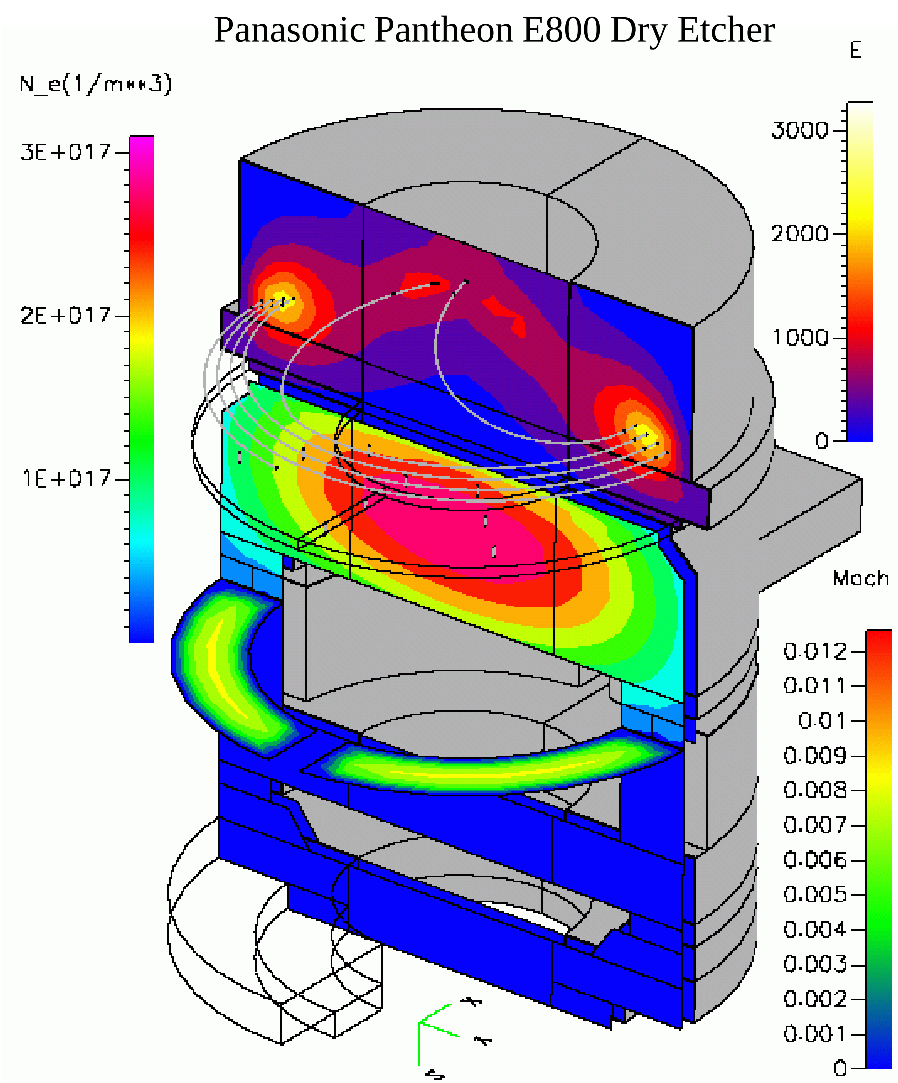

3D simulations of an industrial ICP reactor with comparison to experimental data by V.Kolobov, K.Ikeda and T.Okumura

- Performed simulations of numerous plasma reactors and processes for semiconductor manufacturing, lighting and other applications

- Accumulated considerable experience in developing chemical reaction mechanisms:
  - rare gases (lighting, PDP)
  - O_2, N_2, Cl_2, H_2
  - Fluorocarbon plasmas (SF_6, C_2F_6, ..)
  - SiH_4 for deposition of SiO_2
  - Hydrocarbon plasmas (DLC films, CNT, etc)

- Performed coupled reactor/feature scale simulations using CFD-TOPO

- Developed concept of Virtual Plasma Reactor for process optimization in semiconductor manufacturing

Evolution of Mesh Technologies

- **Partial Differential Equations governing Plasma Dynamics are solved numerically using computational mesh**
- **From Body Fitted Mesh (Structured and Unstructured) to Adaptive Cartesian Mesh with Embedded Boundaries**

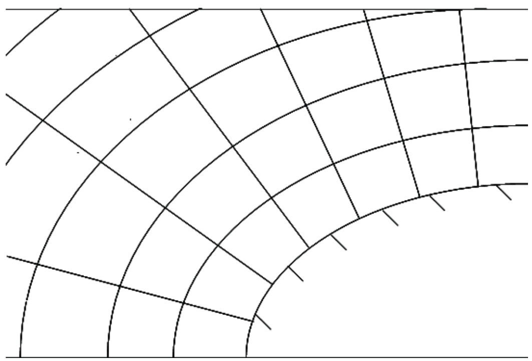

Structured body-fitted rectangular mesh

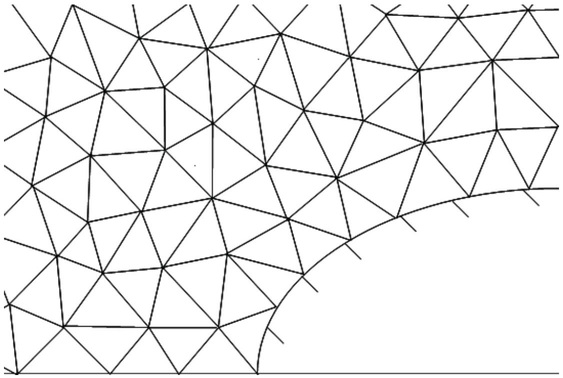

Unstructured body-fitted mesh

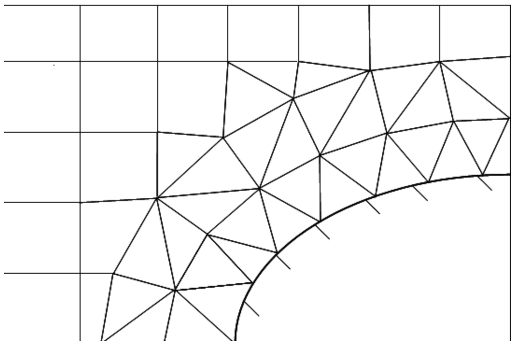

Combination of structured Cartesian mesh and hybrid unstructured body-fitted mesh near the wall

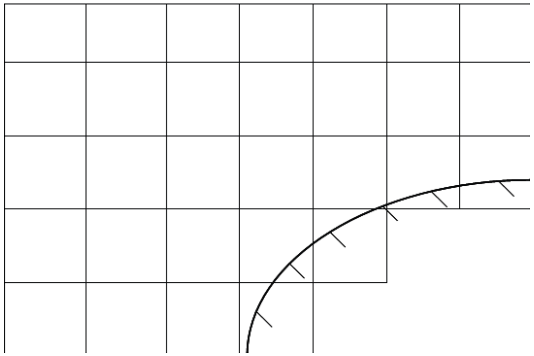

Structured Cartesian mesh with embedded boundary

Comparison of Mesh Types

- **Advantages of body-fitted meshes**
  - **place nodes optimally to resolve geometrical features of the problem**
  - **increase mesh density towards the wall**
- **Disadvantages of body-fitted meshes**
  - **approximation errors caused by spread of inter-nodal distances (LTE)**
  - **loss of robustness caused by skewed faces**
  - **difficulties with automated mesh generation and adaptation**

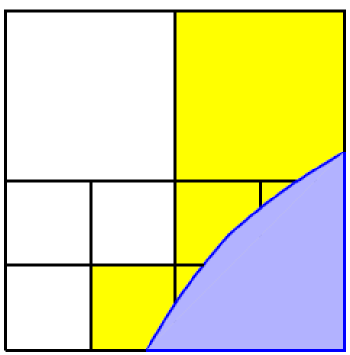

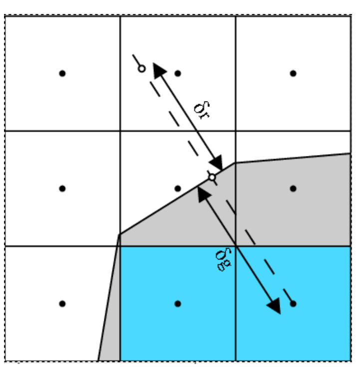

- **Advantages of Cartesian meshes**
  - **Local Truncation Error (LTE) minimization**
  - **robustness of differencing scheme**
  - **simplicity and robustness of mesh generation algorithm**
  - **simplicity of navigation on mesh**
  - **dynamic mesh adaptation**
  - **multi-grid solvers**
- **Drawbacks of Cartesian meshes**
  - **more complicated boundary treatment: cut cells versus Immersed Boundary Methods**

The Future of CFD

CFD and CAD companies are moving towards Cartesian mesh for automatic mesh generation

CONVERGE™ employ a *runtime grid generation* technique for combustion simulations

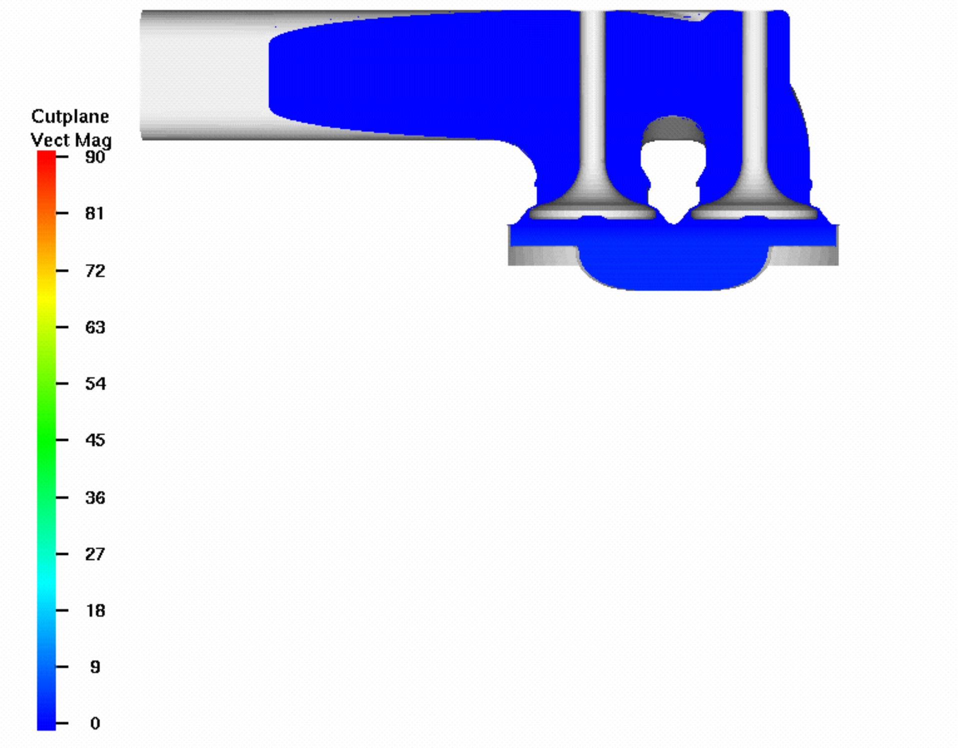

- Eliminates the user-time to generate grids - only the surface geometry is supplied to the CONVERGE™ solver.
- Allows moving boundaries to be handled completely automatically.
- Eliminates the deforming mesh issues typically associated with moving boundaries.
- Allows for perfectly orthogonal cells resulting in improved accuracy and simplified numerics.
- Maintains the true geometry, independent of the mesh resolution. Therefore, the use of fixed embedding or adaptive mesh resolution on boundaries increases the accuracy of the geometry representation.

Open Source CFD: Gerris Flow Solver

- **GFS is a free software for solving PDEs with AMR**
  - Import STL surface geometry from CAD
  - Cut-cell methods to define BC
  - Some moving boundary capabilities

- **Fully Threaded Three for navigation on Mesh**
- **Multi-Grid Poisson Solver**
  - Poisson equation is solved using a relaxation operator
  - Multilevel acceleration is used with a classical “V-cycle”

- **Advection Tracer Solver**
  - Conservative formulation with Godunov scheme for the advection term in the tracer solver
  - The diffusion term is treated using the multigrid Poisson solver

Unified Flow Solver

CFDRC Delivering Breakthrough Solutions

AFRL DSRC DoD Supercomputing Resource Center

- Developed at CFDRC in 2003-2007 as a result of successful U.S. Air Force SBIR (TPOC Eswar Josyula)
- Actively being developed with funding from U.S. Air Force, MDA, NASA, and U.S. Navy

Next Generation Computational Tool for High-Altitude Aerothermodynamics and Low-Speed Micro-Flows

Coupled Continuum and Rarefied Flow Solver Capable of Auto- Switching Based on Local Gradients of Gas Density, Flow Velocity, & Temperature

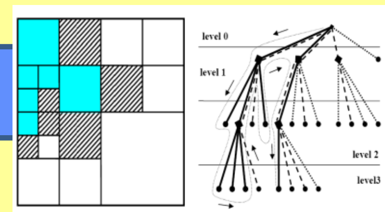

Problem Statement

- A large variety of flow problems are characterized by the presence of continuum and rarefied flow domains
- Computational simulations to define and resolve physical phenomena require appropriate models for both domains
- Direct Simulation Monte-Carlo (DSMC) methods produce statistical scatter so large compared to the small changes of flow quantities that meaningful results can not be obtained

Our Solution

- UFS has been developed for simulations of rarefied, transitional and continuum flows based on direct numerical solution of the Boltzmann equation coupled to kinetic schemes of gas dynamics
- Tree-based, dynamically adaptive mesh, and a local algorithm switching strategy. Quad/Octree Cartesian Mesh is generated by subsequent division of square boxes. The procedure of grid generation is represented by a tree
- Code developed for maximum computational efficiency, with high accuracy and numerical stability

UFS Components

Boltzmann Equation → Direct Simulation Monte Carlo (DSMC); Direct Numerical Solution (DNS)

Domain Decomposition

Coupling Algorithm

Continuum Kinetic Schemes

Adaptive Mesh & Algorithm Refinement

- Automatic generation of Cartesian mesh with embedded solid boundaries
- Tree based adaptation of the mesh to the solution and geometry
- Automatic switching based on continuum breakdown criteria

Key Features

- Direct Numerical Solver (DNS) of the Boltzmann Equation is used in regions of moderate and high local Knudsen number, while kinetic schemes of gas dynamics are used elsewhere
- Direct solver for BTE with different interaction potentials
- Explicit solver for the kinetic Euler and NS equations
- Compact, flexible problem definition & case set-up, with Spatially-varying boundary and initial conditions through input file

High efficiency and numerical stability are attained by using similar computational techniques for kinetic and continuum solvers, and by employing an intelligent domain decomposition algorithm

Applications

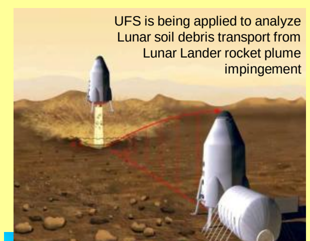

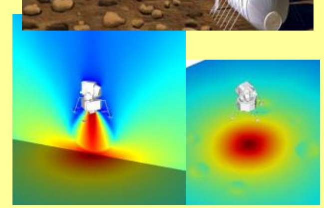

UFS provides a push-button tool for generating a deterministic ensemble of steady-state and tumbling body aerodynamic datasets of Missile Debris Fragments enabling more accurate probability of kill predictions

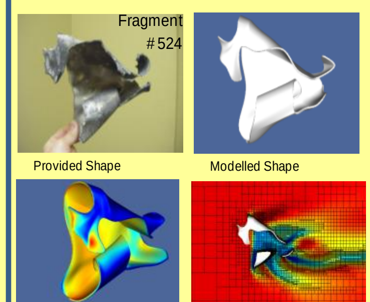

Provided Shape | Modelled Shape | Surface Pressure Distribution | Fully resolved Mach No. Contours

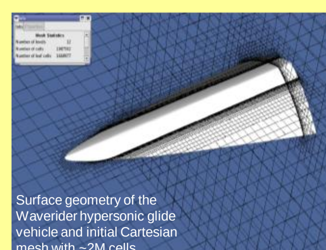

Surface geometry of the Waverider hypersonic glide vehicle and initial Cartesian mesh with ~2M cells

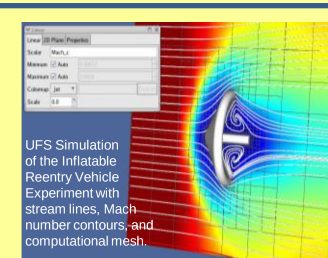

UFS Simulation of the Inflatable Reentry Vehicle Experiment with stream lines, Mach number contours, and computational mesh.

Illustration of UFS methodology

Dynamic mesh adaptation to the solution and automatic selection of fluid or kinetic solvers based on continuum breakdown criteria

Flow Around Cylinder for different Kn numbers: M=3, Tw=4

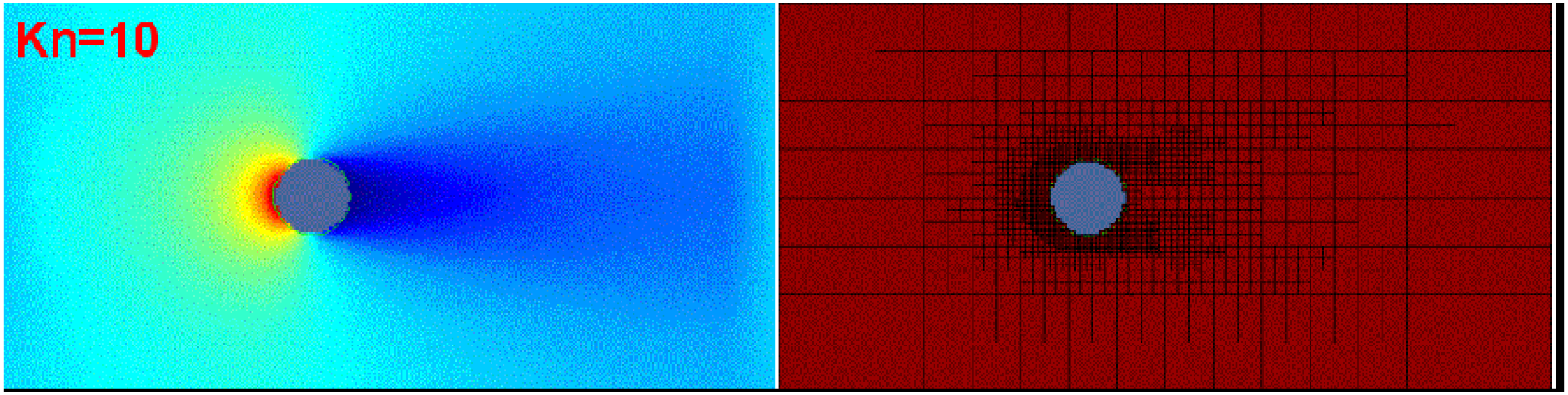

Density Profile

Continuum Breakdown Criterion:

Mesh Refinement Criterion:

$$\nabla \rho < \varepsilon = 0.1$$

$$Kn\sqrt{\left(\frac{\nabla p}{p}\right)^2 + \frac{1}{T}\left[\left(\frac{\partial u}{\partial x}\right)^2 + \left(\frac{\partial \upsilon}{\partial y}\right)^2\right]} < \delta = 0.1$$

Cartesian Mesh with Cut Cell Embedded Boundary

Space Filling Curves for Parallelization

Domain decomposition using SFC

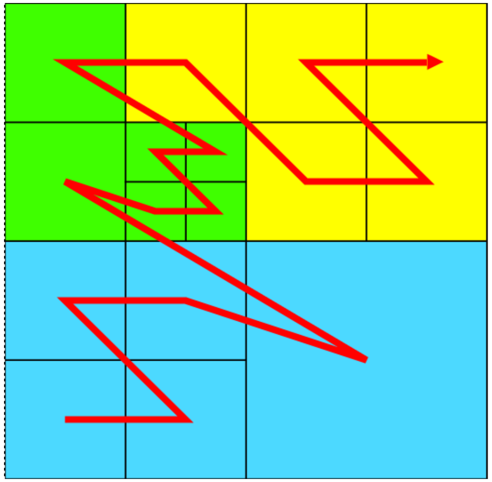

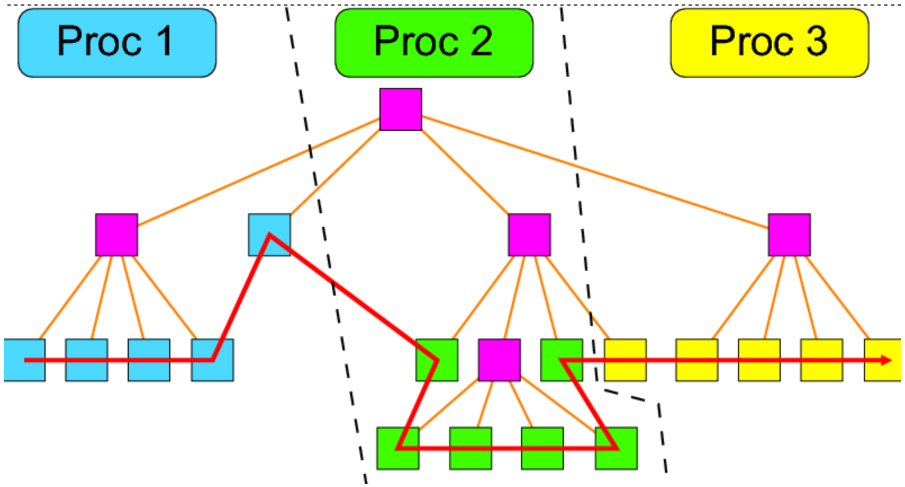

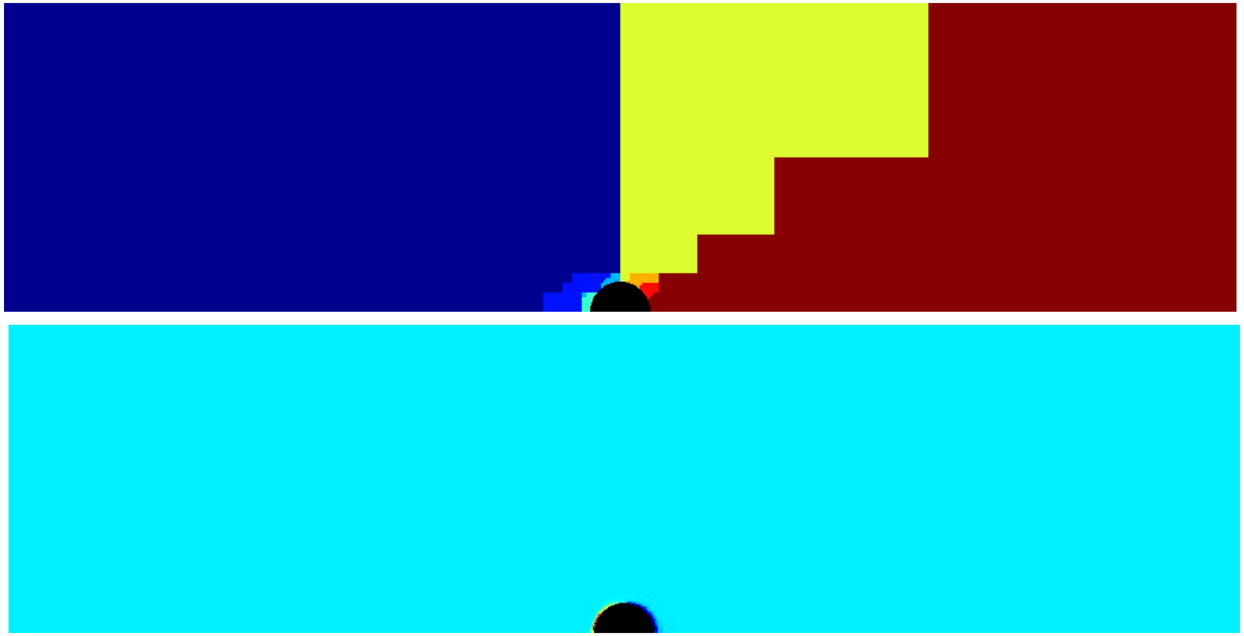

Illustration of Dynamic Load Balancing

Plasma Modeling with AMR

Minimal Plasma Model

A simplest set of equations for the electron and ion densities, and Poisson equation for electrostatic potential.

Electron diffusion and ion transport are neglected

$$\frac{\partial n_e}{\partial t} + div\left(\vec{\Gamma}_e\right) = \nu n_e \qquad \vec{\Gamma}_e = \mu \vec{E} n_e$$

$$\frac{\partial n_i}{\partial t} = \nu n_e$$

$$\nu = \nu_0 \exp\left[-\frac{E_0}{E}\right]$$

$$\Delta\varphi = 4\pi\left(n_e - n_i\right)$$

Mesh Adaptation criteria

$$\alpha = 20\left(\frac{n_e}{\max(n_e)} + \frac{n_e}{\max(n_e)}\right) + 3\left(\log_{10}(n_e) + \log_{10}(n_i) + \log_{10}(\nu_i) + \log_{10}(|E|)\right)$$

When gradient of α exceeded a fixed value $|\nabla\alpha| > 1$ in a cell, this particular cell was refined

When $|\nabla\alpha| < 1/4$ in a cell, this cell was coarsened

The procedure of mesh adaptation performed after several time steps

Streamer development in negative corona

2D axi-symmetric simulation of streamer development near a needle-like elliptic cathode and a flat anode: *p*=760 Torr

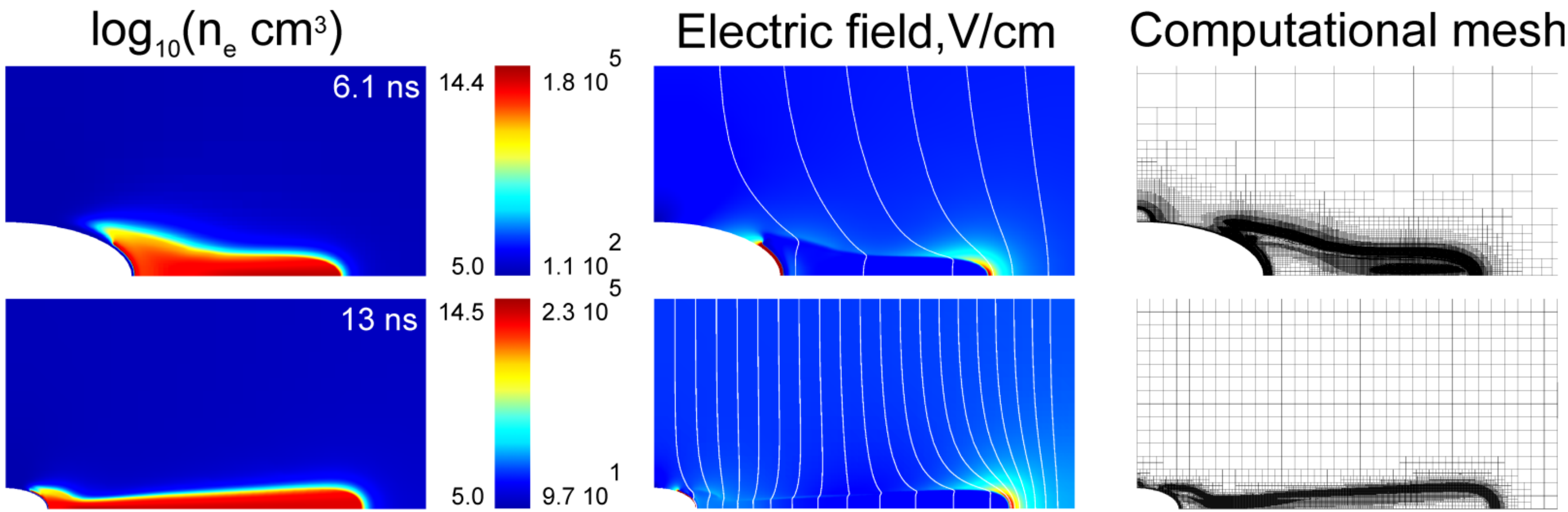

A constant electron density 10^5 cm^{-3} is assumed at the cathode surface. The streamer propagates with a velocity by an order of magnitude higher than the electron drift velocity .

The calculated streamer velocity agrees with the classical estimate for the fast streamer velocity.

The plasma channel is formed on the axis of the discharge.

Streamer development in positive corona

2D axisymmetric simulations of positive corona discharge

An off-axis toroidal channel was formed in our simulations.
This behavior was observed with different physical models for different electrode shapes.

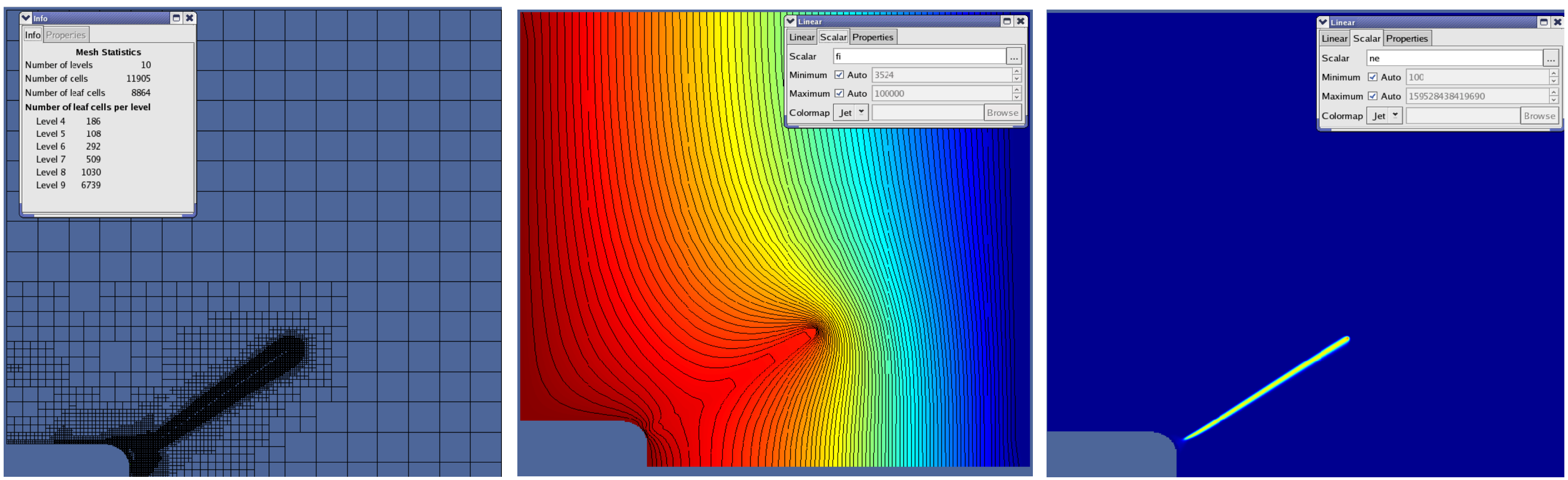

The computational grid (left), electrostatic potential (center), and the electron density (right) for a streamer developing near a rod-shape anode.

3D structures in positive corona

3D simulations revealed that the 2D axi-symmetric channels break into separate streamers. The streamers form near the anode with an almost periodic pattern and propagate in slightly different directions with different speeds. Only two streamers survived at a long distance from the anode. The code generates about 1.5 million cells during parallel simulations on 8 cores.

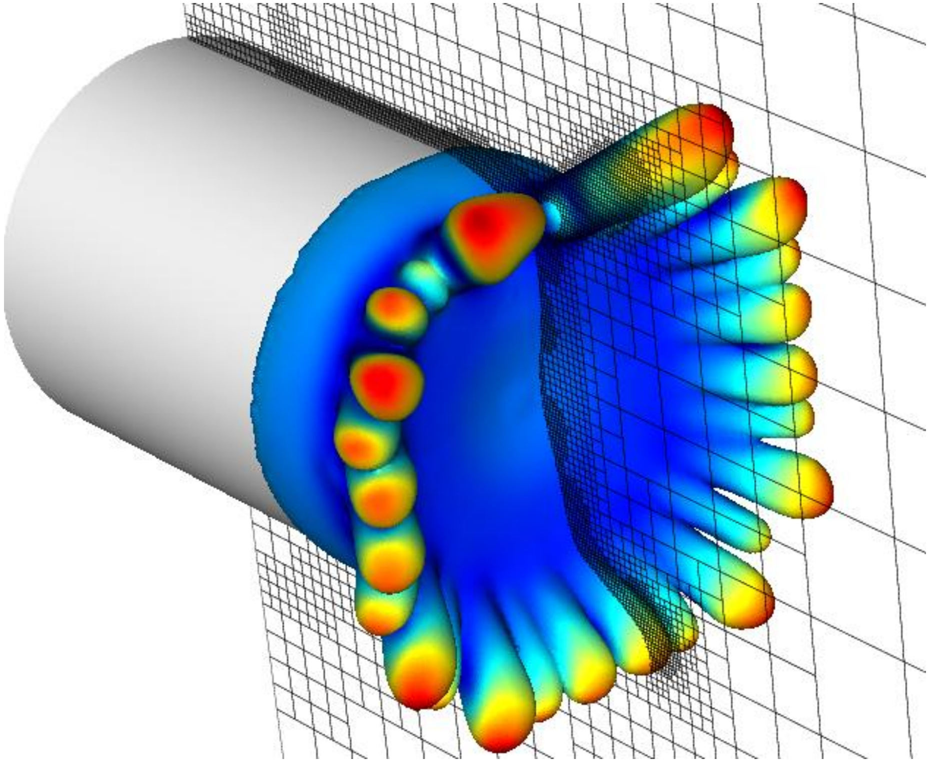

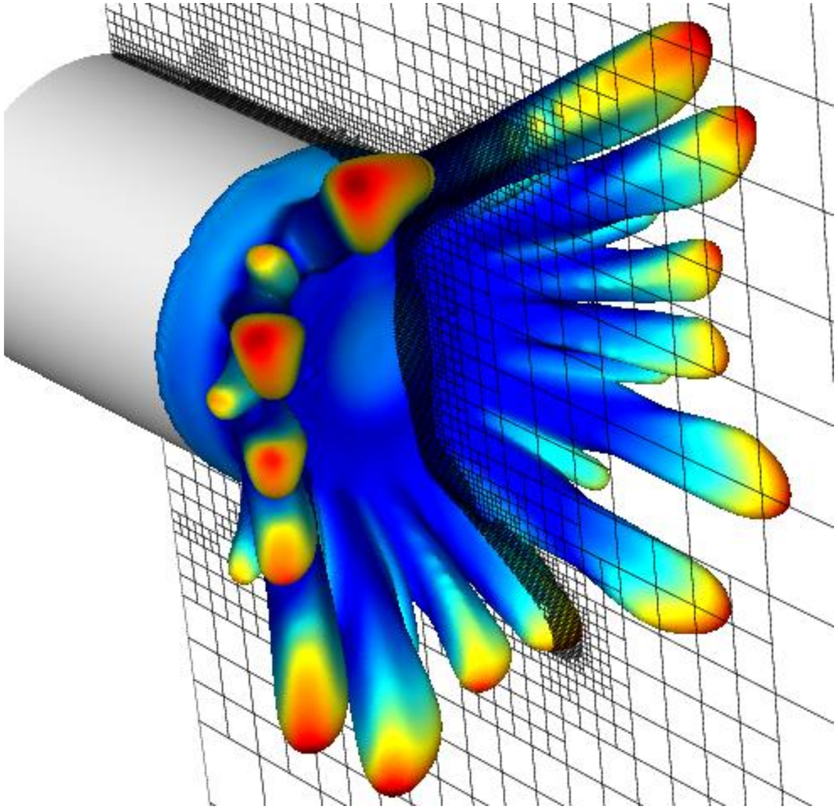

Computational grid, electron density contours at 10^7 cm $^{-3}$, and the electric field strength (color, maximum value $7\ 10^6$ V/m) at 15 ns (left) and 20 ns (right)

Extended Plasma Model

- A set of equations for the electron and ion densities, and Poisson equation for electrostatic potential

$$\frac{\partial n_e}{\partial t} + div\left(\vec{\Gamma}_e\right) = \nu n_e$$

$$\vec{\Gamma}_e = -\mu_e \vec{E} n_e - D_e \nabla n_e$$

$$\Delta\varphi = 4\pi\left(n_e - n_i\right)$$

- Ion transport is included

$$\frac{\partial n_i}{\partial t} + div(\Gamma_i) = \nu n_e$$

- Multiple species ions are allowed by introducing species specific mass, diffusion coefficients, and ionization rates

$$\vec{\Gamma}_i = \mu_i \vec{E} n_i - D_i \nabla n_i$$

- Local field approximation for ionization rate

$$\nu = \nu_0 \exp\left[-\frac{E_0}{E}\right]$$

- Electron Energy Transport with account for electron thermal conductivity

$$\frac{\partial n_\varepsilon}{\partial t} + \nabla \cdot \vec{\Gamma}_\varepsilon = S_\varepsilon \qquad n_\varepsilon = n_e \overline{\varepsilon}$$

- CANTERA link implementation is underway for complex reaction mechanisms

$$\vec{\Gamma}_\varepsilon = -\frac{5}{3}\mu_e \vec{E} n_\varepsilon - \frac{5}{3} D_e \nabla n_\varepsilon$$

Classical DC Glow Discharge

2D axi-symmetric simulations

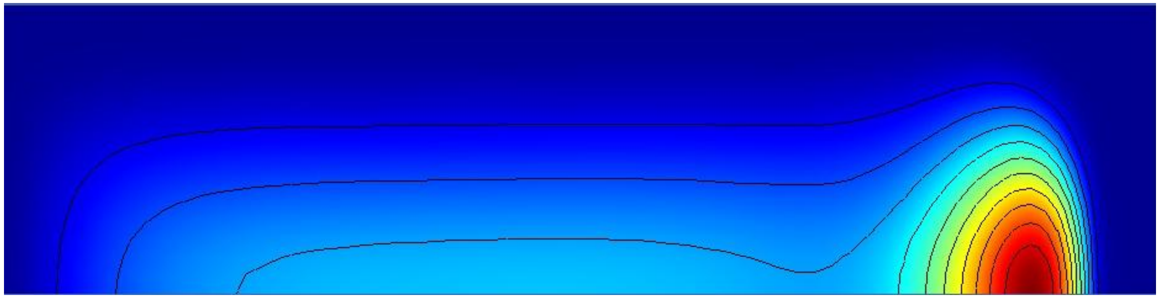

The model reproduces basic structure of classical DC glow discharges

Spatial distribution of electron density with account of thermal conductivity

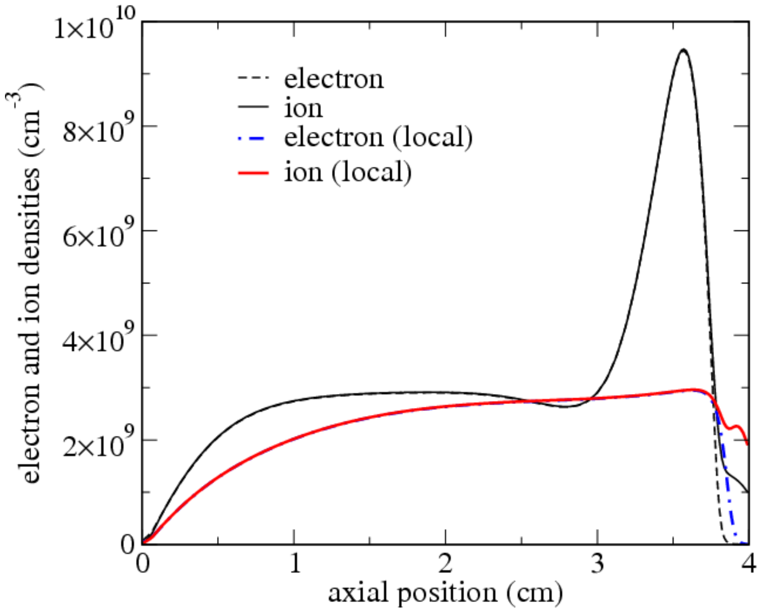

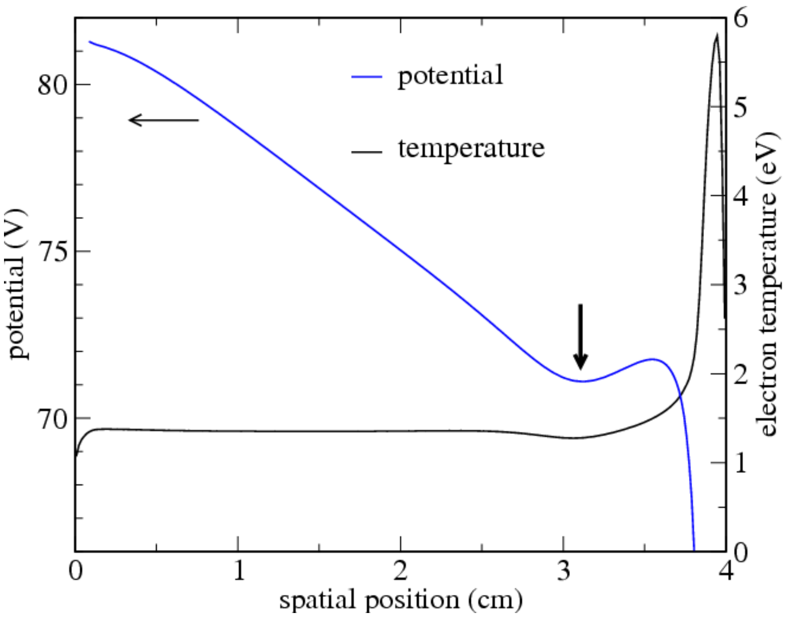

Axial distributions of electron and ion densities (left), electrostatic potential and electron temperature (right) with account of electron thermal conductivity

Discharges with Rod Shape Cathode

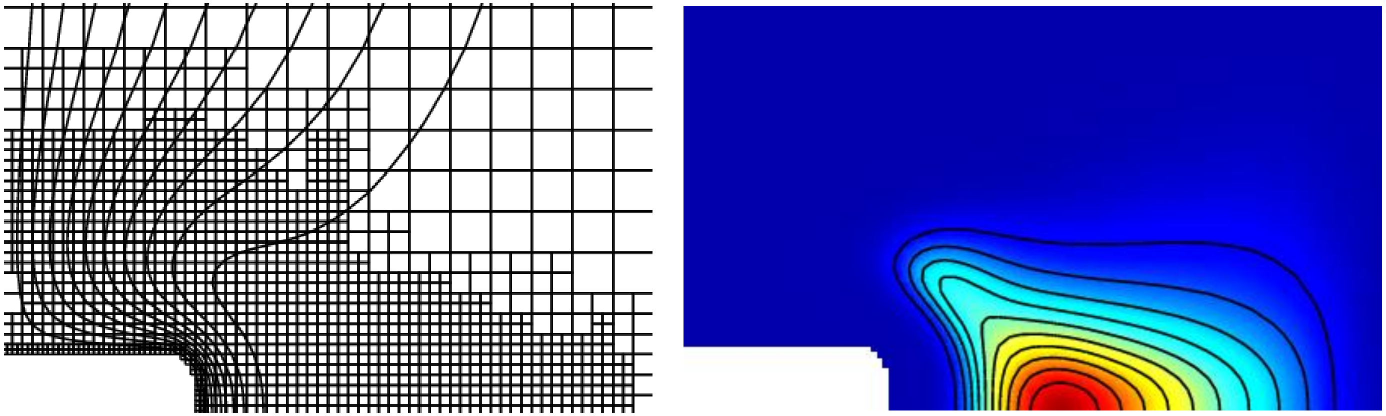

15 Torr
32 μA

Computational grid and the electrostatic potential (left), and electron density contours (right) for a glow discharge between a rod cathode and a planar anode.

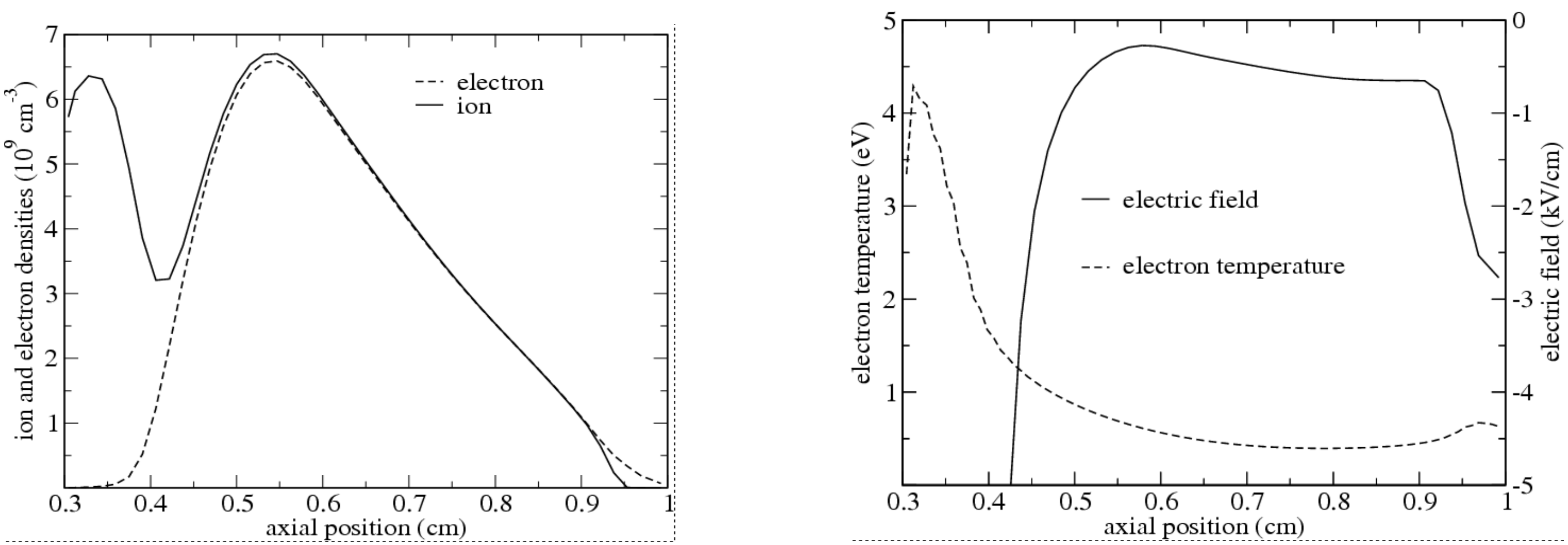

Axial profiles of the electron and ion density (left), the electron temperature and the x-component of the electric field (zoom on the plasma region)

Cage Discharge

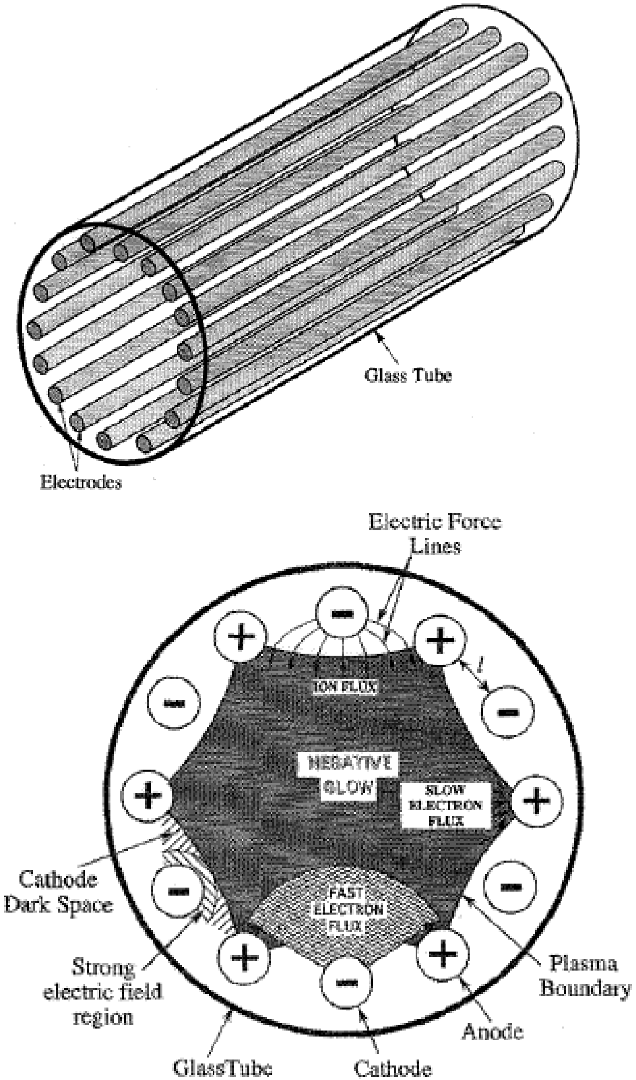

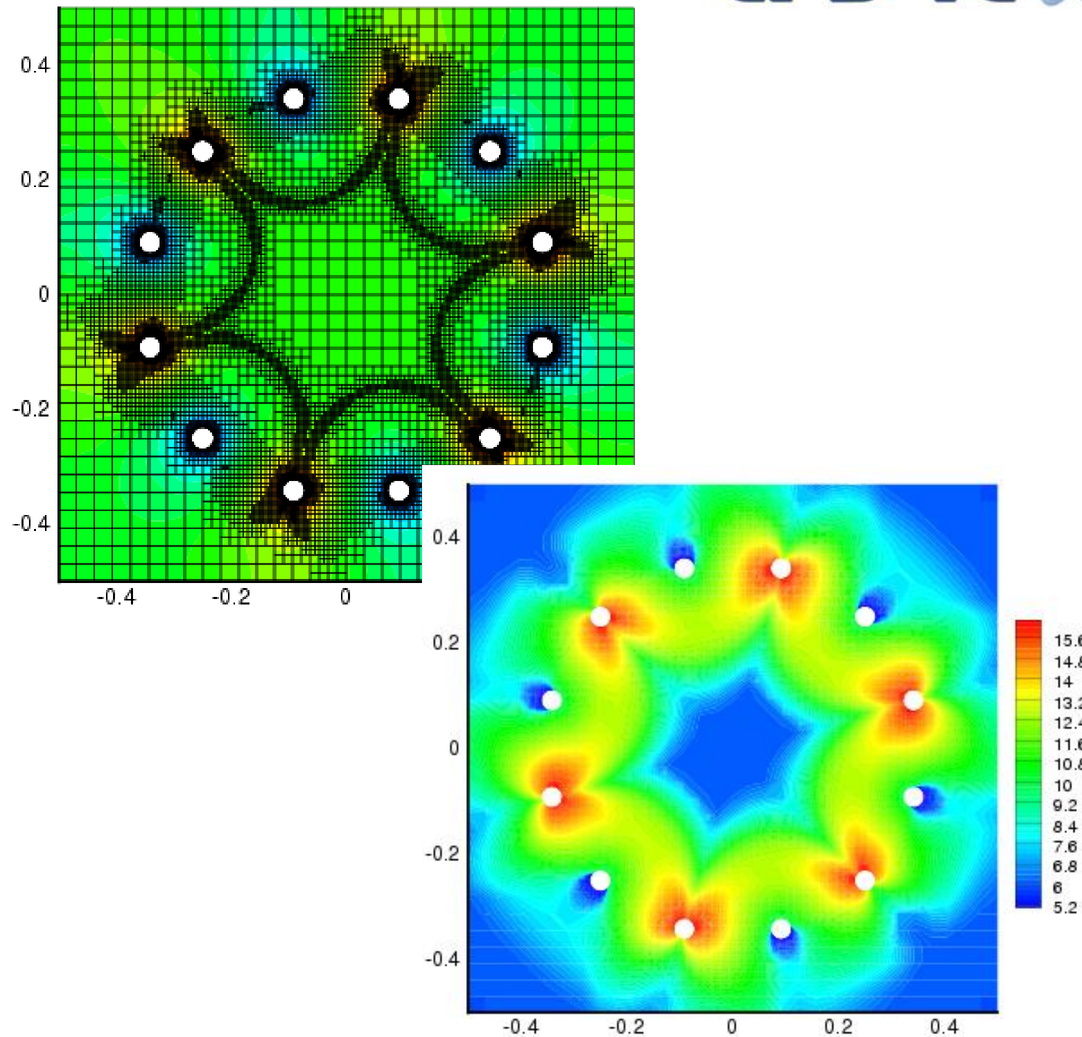

Schematic of cage discharge and discharge cross section illustrating high-density plasma generation process (right).

Computational grid and electric potential and $log_{10}(n_e)$ (right) for a cage discharge

Conclusions & Future Plans

• 3D simulations of industrial plasma reactors can be routinely done today using fluid models

• Adaptive Cartesian mesh has many advantages compared to the traditional body-fitted mesh techniques

• We have developed a Unified Flow Solver using AMAR technique for coupling kinetic and fluid solvers for gas flows

• We have shown that fluid plasma models can be extended for the adaptive Cartesian mesh and illustrated the benefits of AMR for simulations of corona and streamer discharges

• The development of adaptive kinetic-fluid simulations of plasmas is a subject of our current research

Acknowledgement

• Work supported by a NASA SBIR Project and AFOSR STTR Projects.

• Further details can be found in Kolobov & Arslanbekov "Towards Adaptive Kinetic-Fluid Models of Weakly Ionized Plasmas", Journal of Computational Physics, doi:10.1016/j.jcp.2011.05.036